

# The reliability of low-dose chest CT for the initial imaging of COVID-19: comparison of structured findings, categorical diagnoses and dose levels

Hakkı Muammer Karakaş 

Gülşah Yıldırım 

Esin Derin Çiçek 

## PURPOSE

The widespread use of computed tomography (CT) in COVID-19 may cause adverse biological effects. Many recommend to minimize radiation dose while maintaining diagnostic quality. This study was designed to evaluate the difference between findings of COVID-19 pneumonia on standard and low-dose protocols to provide data on the utility of the latter during initial imaging of COVID-19.

## METHODS

Patients suspected of having COVID-19 were scanned with a 128-slices scanner using two consecutive protocols in the same session (standard-dose scan: 120 kV and 300 mA; low-dose scan: 80 kV and 40 mA). Dose data acquisition and analysis was performed using an automated software. High and low-dose examinations were anonymized, shuffled and read by two radiologist with consensus according to a highly structured reporting format that was primarily based on the consensus statement of the RSNA. Accordingly, 8 typical, 2 indeterminate, and 7 atypical findings were investigated. Cases were then assigned to one of the categories: (i) Cov19Typ, typical COVID-19; (ii) Cov19Ind, indeterminate COVID-19; (iii) Cov19Aty, atypical COVID-19; (iv) Cov19Neg, not COVID-19. McNemar test was used to analyze the number of disagreements between standard and low-dose scans regarding paired proportions of structured findings. Inter-test reliability was tested using kappa coefficient.

## RESULTS

The study included 740 patients with a mean age of  $44.05 \pm 16.59$  years. The median (minimum–maximum) dose level for standard protocol was 189.98 mGy·cm (98.20–493.54 mGy·cm) and for low-dose protocol was 15.59 mGy·cm (11.59–32.37 mGy·cm) differing by -80 and -254 mGy·cm from pan-European diagnostic reference levels. Only two findings for typical, one finding for indeterminate, and three findings for atypical categories were statistically similar ( $p > 0.05$ ). The difference in other categories resulted in significantly different final diagnosis for COVID-19 ( $p < 0.001$ ). Overall, 626 patients received matching diagnoses with the two protocols. According to intertest reliability analysis, kappa value was found to be 0.669 ( $p < 0.001$ ) to indicate substantial match. CT with standard-dose had a sensitivity of 94% and a specificity of 72%, while CT with low-dose had a sensitivity of 90% and a specificity of 81%.

## CONCLUSION

Low kV and mA scans, as used in this study according to scanner manufacturer's global recommendations, may significantly lower exposure levels. However, these scans are significantly inferior in the detection of several individual CT findings of COVID-19 pneumonia, particularly the ones with GGO. Therefore, they should not be used as the protocol of choice in the initial imaging of COVID-19 patients during which higher sensitivity is required.

Department of Radiology (H.M.K. ✉ [hakki.karakas@gmail.com](mailto:hakki.karakas@gmail.com), G.Y., E.D.Ç.), University of Health Sciences, Istanbul Fatih Sultan Mehmet Training and Research Hospital, Istanbul, Turkey.

Received 1 October 2020; revision requested 4 November 2020; last revision received 5 March 2021; accepted 12 March 2021.

Published online 7 May 2021.

DOI 10.5152/dir.2021.20802

**S**evere acute respiratory syndrome coronavirus-2 (SARS-CoV-2) is transmitted from person to person, mainly by respiratory droplets and surface contact, with high incidence, high concealment, and rapid transmission (1). Patients may become a source of infection not only when they are symptomatic but also during the incubation or the recovery period (2). Coronavirus disease 2019 (COVID-19), the pneumonia that is caused by SARS-CoV-2, has therefore become a serious worldwide public health threat. Accurate and timely diagnosis of the disease is critical for effective treatment, better survival, and control of disease spread. Currently, COVID-19 pneumonia is diagnosed by the reverse transcriptase-polymerase chain reaction (RT-PCR) test. However, the high false-negative rate for the

You may cite this article as: Karakaş HM, Yıldırım G, Çiçek ED. The reliability of low-dose chest CT for the initial imaging of COVID-19: comparison of structured findings, categorical diagnoses and dose levels. *Diagn Interv Radiol* 2021; 27: 607–614

disease of up to 60% and the unavailability of instant results create a real clinical problem where positive cases must be identified and isolated to prevent disease transmission to healthy individuals (3).

Chest computed tomography (CT) is a rapid and effective imaging tool for COVID-19 pneumonia with high sensitivity of up to 95% due to so-called typical CT findings of the disease (4, 5). Experts, therefore, formed a temporary consensus on CT being a major tool in diagnosing COVID-19 (6). That consensus was later supported by the World Health Organization (WHO), which acknowledged imaging as one element of the diagnostic workup of patients with suspected or probable COVID-19 disease where RT-PCR is not available, results are delayed or are initially negative in the presence of symptoms suggestive of COVID-19 (7). CT has also been considered to complement clinical and laboratory evaluation in the management of patients already diagnosed with COVID-19 (7). However, the relatively high level of ionizing radiation inherent to the technique may cause adverse biological effects on humans (8, 9). Therefore, many authorities and experts, including the WHO, recommend minimizing the radiation dose while maintaining diagnostic image quality when performing chest CT and adjusting protocols to reduce exposure while maintaining quality (7).

Lowering the dose is a complex and comprehensive task that encompasses whole imaging cycle including the use CT equipment that meet lower dose criteria, availability of modern dose reduction algorithms, standardization of protocol and strict adherence to and uniformity of scanning technique (10, 11). Optimization, the subprocess to lower protocol dose length

products (DLPs) with regard to the initial diagnostic reference levels (DRLs), is even more challenging as it is limited by the ALARA (as low as reasonably achievable) principle. Thus, any such attempt must not decrease the diagnostic ability of the imaging system for the particular indication that the system is used for. Although, COVID-19 is a novel disease, many studies have been conducted to date and typical, indeterminate and atypical CT features of the disease have been described (12). Also there are some non-comparative studies where diagnostic performance of low-dose chest CT to detect COVID-19 was investigated (13). This study, therefore, was designed to comparatively evaluate the diagnostic ability of standard-dose CT and low-dose CT in detecting COVID-19 features. The goal of the study was to test whether low-dose chest CT could be used during the initial imaging of suspected COVID-19 patients without compromising the diagnostic ability of the imaging modality.

## Methods

### Institution

The study was conducted in a mid-size hospital serving a population of circa 400 000 under normal conditions. The facility served as a pandemic hospital where many patients from other hospitals and districts were referred. The hospital was one of the first institutions in the country where a comprehensive dose management system was implemented and modern dose surveillance applications were used.

### Patients

For the study, data from March 21<sup>st</sup>, 2020 to April 2<sup>nd</sup>, 2020 was evaluated. First case in the country was recorded on March 11<sup>th</sup>, 2020. At that time, the Fleischner Society Consensus Statement was not yet published and at our institution, CT imaging was mainly performed for the medical triage of patients with suspected COVID-19 who were presented with moderate-severe clinical features and a high pretest probability of disease (14). However, there were few cases where it was used for suspected COVID-19 and mild clinical features. During the period, 1753 patients were admitted with symptoms suggestive of COVID-19 infection and 1032 of them were referred to CT and RT-PCR. These patients were scanned immediately after being sampled with oropharyngeal and nasal swabs

during their initial admission to emergency clinic. Of these, only 708 patients granted informed consent to the study and were scanned with both standard-dose and low-dose protocols due to clinical and operational constraints and had technically adequate CT images. During the specified time period, the frequency and the relative frequency of RT-PCR proven cases were low and 32 RT-PCR proven COVID-19 patients who were scanned at a later period were added to the above described cohort to increase statistical power (Fig. 1). Therefore, the final study group consisted of 740 patients (437 male [59.1%] and 303 female patients [40.9%]) aged between 18 and 97 years (44.05±16.59 years). This study was approved by the institutional review board (Approval no: 2020-06-15T13\_54\_27 and 09-07-2020/87) and informed consent was obtained from all participants.

### Scanner and dose-tracking

Sequences were acquired with a 128-slices scanner (Optima 660 SE, GE Healthcare). The equipment met XR-29 lower dose criteria. The system had adaptive statistical iterative reconstruction technology (ASIR, GE Healthcare) that extracts noise by photon statistics and object modelling. Patients were scanned with two protocols consecutively on the same session. These included a standard-dose scan with 120 kV and 300 mA exposure and a low dose scan with 80 kV and 40 mA exposure as recommended by the scanner's manufacturer. All parameters, including scan plane and the coverage were identical except kV and mA values and statistical reconstruction factor to compensate noise level during low exposure acquisition (Table 1). Imaging was performed with the patient in supine position, with both hands raised above the head, scanning from the apex of both lungs to the diaphragm during deep inspiration.

For dose data acquisition and analysis, a commercial software (DoseWatch, GE Healthcare) was used. This software captures, tracks and reports radiation dose directly from the medical devices and it includes quality metrics to assess technical factors. The application was provided with patients' height and weight to calculate size-specific dose estimates (SSDE) (15). Conventional dose data (CTDIvol and DLP) were recorded and calculated. Basic dose statistics based on protocol (DLP, minimum, P25, median, P75, maximum) were automatically determined for all available

### Main points

- Widespread use of CT in the diagnosis and follow-up of COVID-19 raised concerns on theoretical acute radiation damage and possible long-term stochastic effects in patients.
- There is almost a 14-fold difference between manufacturer's suggested standard-dose and low-dose protocols in terms of calculated patient dose.
- Submillisievert scans have high sensitivity (90%) and specificity (81%).
- Low-dose chest CT may not be used in the initial imaging of patients during COVID-19 pandemic where high sensitivity is preferred.

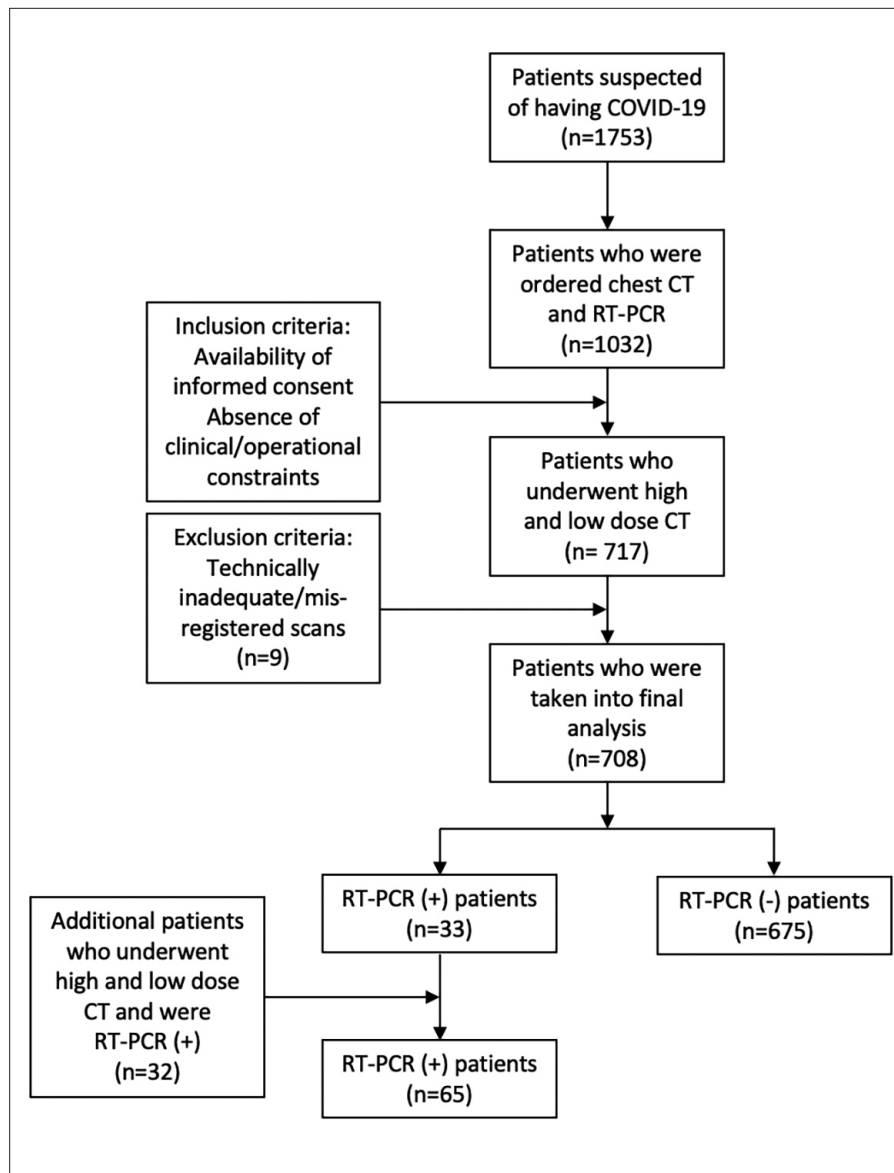


Figure 1. Flowchart for patient selection.

Parameters	Standard-dose	Low-dose
Rotation (s)	0.6	0.5
Thickness (mm)	5.0	5.0
Speed	1.375	1.375
Interval (mm)	5.0	5.0
Tube voltage (kV)	120	80
Tube current (mA)	300	40
Total exposure time (s)	~4.62	~3.53
Dose efficiency (%)	95.61	95.61
FOV (mm)	500	500
Matrix (pixel)	512×512	512×512
Statistical reconstruction (%)	40	80

CT, computed tomography; COVID-19, coronavirus disease 2019; FOV, field of view.

patients. Detailed dose information such as SSDE, effective dose, and detailed protocol parameters were also recorded or calculated. Off-isocenter shift to identify how the patient was positioned in the bore of the CT and mA modulation to visually observe how dose was optimized along the patient scan length were also presented to determine the optimality of technical parameters. Differences of DLP for standard-dose and low-dose protocols were compared with the hospital's published DLP (168 mGy·cm) and the unified pan-European DRLs (270 mGy·cm) based on published data from several European countries (11, 16, 17).

### Structured reporting

Standard-dose and low-dose examinations were anonymized and shuffled by a randomization process. They were read in consensus by two senior radiologists who were blinded to the identities of patients and their clinical and/or laboratory findings. Standard-dose studies were also officially read by another team of radiologists. The findings of this study were not used for official reports or for patient management.

All exams were read on DICOM calibrated 3 MP diagnostic monitors (EMX 16, Eizo) at fixed window level of -450 HU and window width at 1600 HU using 5.0 mm and 1.2 mm axial reconstructions. A highly structured reporting format that was primarily based on the consensus statement of the Radiological Society of North America (RSNA) that classified the CT appearance of COVID-19 into four categories for standardized reporting language was used (12). Accordingly, eight typical, two indeterminate, and seven atypical findings were sought. Five of the typical and four of the atypical findings were taken directly from the consensus statement and they are considered as primary findings. Three secondary findings for typical and another three for atypical presentations were also noted as appropriate (Table 2) (18). These secondary findings, however, were not used for the final diagnosis. All findings were recorded as present (Yes) or not present (No) for each parameter. Cases were then assigned to one of the categories below: (i) Cov19Typ, typical findings of COVID-19 pneumonia; (ii) Cov19Ind, indeterminate findings of COVID-19 pneumonia; (iii) Cov19Aty, atypical findings of COVID-19 pneumonia; (iv) Cov19Neg, no findings of COVID-19 pneumonia (12).

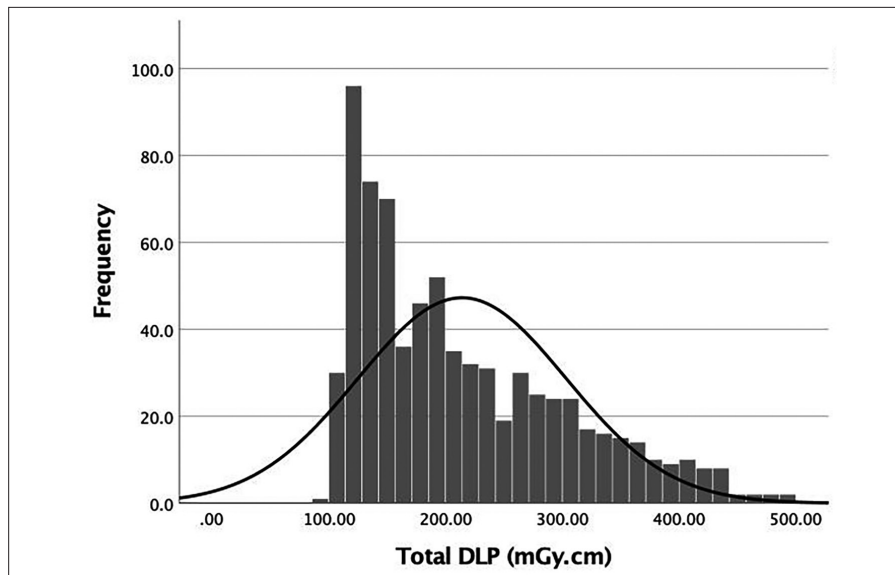


**Figure 2.** Distribution of total dose length products (DLPs) in scans with standard-dose and the normal distribution curve.

**Table 2.** Categorical findings for structured reporting of COVID-19 and their codes as used in the article

Category	Subcategory	Finding
Typical	Primary	Peripheral bilateral/multilobar GGO
		Multifocal rounded GGO
		Reverse halo
		Consolidation
		Crazy-paving
	Secondary	Bronchovascular enlargement
		Air bronchogram
		Bronchial deformation
Indeterminate	Primary	Multifocal/diffuse/perihilar/unilateral GGO with or without consolidation
		Nonrounded and non-peripheral few very small GGO
Atypical	Primary	Lobar/segmental consolidation without GGO
		Small discrete nodules, tree in bud/centrilobular
		Cavitation
		Effusion
	Secondary	Lymphadenopathy
		Pneumothorax
		Diffuse fibrosis
Negative	Primary	No features to suggest pneumonia

COVID-19, coronavirus disease 2019; GGO, ground-glass opacity.

### Statistical analysis

Statistical evaluation was performed using IBM SPSS Statistics (version 27, IBM). Data were described using exploratory statistical methods. Occurrence of findings were given in frequency (n) and percentage (%). Minimum (min), lower quartile

(P25), median, upper quartile (P75), and maximum (max) values were indicated. The normality of the distribution was evaluated by Kolmogorov–Smirnov statistics, with a Lilliefors correction for testing normality. McNemar test was used to analyze the number of disagreements between stan-

dard and low-dose scans regarding paired proportions of structured findings. Related samples Wilcoxon signed rank test was used for the comparison of the non-normally distributed continuous variables. The Cohen's kappa statistics was used to test intertest reliability.  $p < 0.01$  was chosen as the level of significance.

### Results

The median dose level (DLP) for standard-dose protocol was 189.98 mGy-cm (min, 98.20 mGy-cm; P25, 139.48 mGy-cm; P75, 273.83 mGy-cm; max, 493.54 mGy-cm) (Fig. 2). The median dose level for low-dose protocol was 15.59 mGy-cm (min, 11.59 mGy-cm; P25, 14.79 mGy-cm; P75, 16.39 mGy-cm; max, 32.37 mGy-cm) (Fig. 3). Both protocols showed non-normal distribution. There was a significant difference between both protocols regarding patient dose levels ( $p < 0.001$ ) (Fig. 4). Accordingly, the latter value has represented a reduction of 91.79% in dose level over the standard-dose protocol. The DLP of the standard-dose was higher than our hospital's DLP with a difference of 22 mGy-cm and lower than pan-European unified DRL with a difference of -80 mGy-cm. The DLP of the low-dose, on the other hand, was much lower than both our hospital's DLP and pan-European unified DRL with differences of -152 and -254 mGy-cm, respectively.

Considering the categorical elements of the structured reporting, only six out of 17 categorical findings (multifocal rounded ground-glass opacity [GGO], consolidation, nonrounded and non-peripheral few very small GGO, lobar/segmental consolidation without GGO, pneumothorax) showed no statistically significant difference between standard and low-dose studies ( $p$  values ranging as 1.000–0.052) (Table 3). All other findings were significantly different between the two protocols ( $p < 0.001$ ) (Figs. 5 and 6). Difference in categorical findings resulted in significantly different final diagnoses for COVID-19 (Table 4). Overall, 626 patients out of 740 received matching diagnoses with the two protocols ( $p < 0.001$ ; Table 5). The reliability of low-dose protocol was further tested using Cohen's kappa on final diagnoses. According to this analysis, intertest reliability measure (kappa) was found to be 0.669 ( $p < 0.001$ ). This value was considered substantial according to Cohen's original article, but should be interpreted with caution for a diagnostic test where a

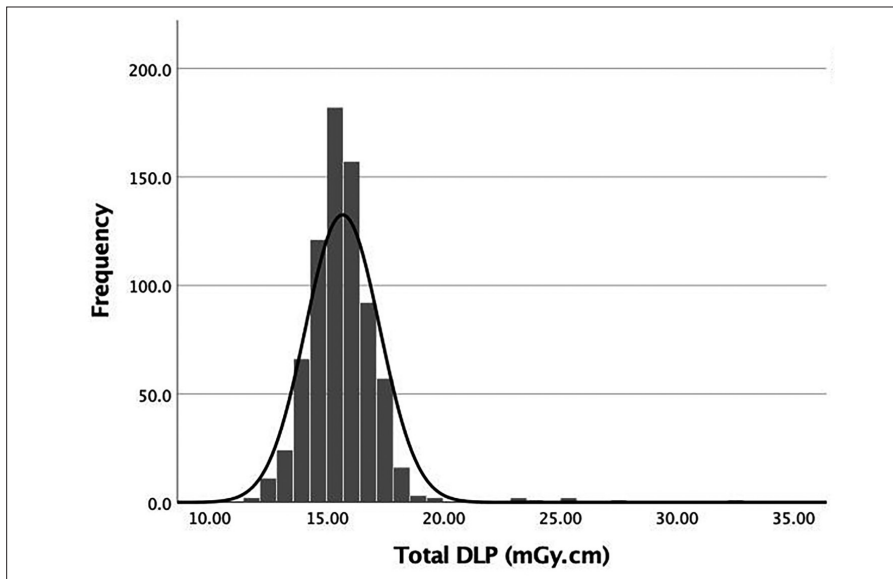


Figure 3. Distribution of total DLPs in scans with low-dose and the normal distribution curve.

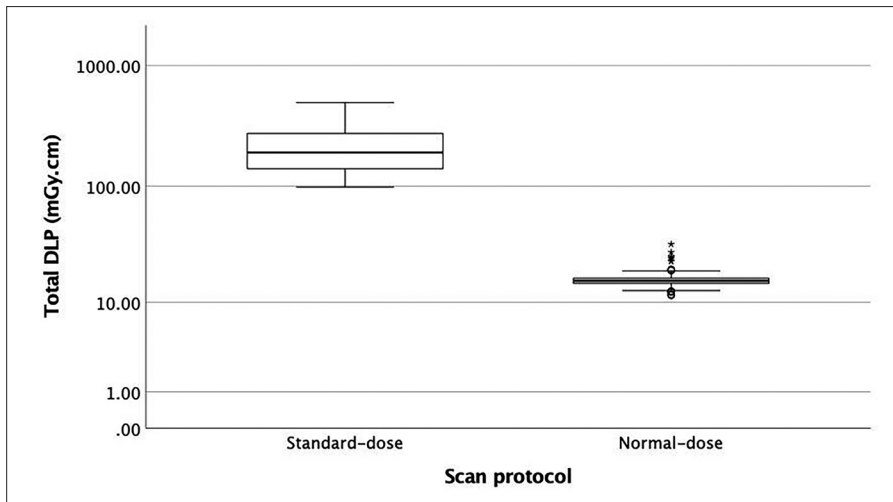


Figure 4. Comparison of median DLPs and their statistical deviations for standard and low-dose protocols.

higher kappa value would be required (19). Among 740 cases that were evaluated in the study, 65 (8.8%) were tested positive for COVID-19 using RT-PCR. The standard-dose protocol correctly identified 61 cases (i.e., true positive). Of these cases, 53 were classified as Cov19Typ and the remaining 8 were classified as Cov19Ind. Four RT-PCR positive cases were classified as Cov19Neg (i.e., false negative). Of RT-PCR negative patients, 482 were correctly identified (i.e., true negative) and remaining 193 were classified as Covi19Typ (n=108), Cov19Ind (n=56) and Cov19Aty (n=29) (i.e., false positive). Therefore, CT with standard-dose protocol had a sensitivity of 94% and a specificity of 72%.

Using the low-dose protocol, 58 of RT-PCR positive cases were correctly identified. Of

these cases, 49 were classified as Cov19Typ, seven were classified as Cov19Ind and two were classified as Cov19Aty. Four RT-PCR positive cases were classified as Cov19Neg. Of RT-PCR negative patients, 547 were correctly identified (i.e., true negative) and remaining 128 were classified as Cov19Typ (n=76), Cov19Ind (n=30) and Cov19Aty (n=22) (i.e., false positive). Therefore, CT with low-dose protocol had a sensitivity of 90% and a specificity of 81%. The difference between CT with standard-dose and low-dose was 4% for sensitivity and -9% for specificity.

## Discussion

COVID-19 requires rapid diagnostic methods to identify and isolate patients. Although RT-PCR is highly specific in diagno-

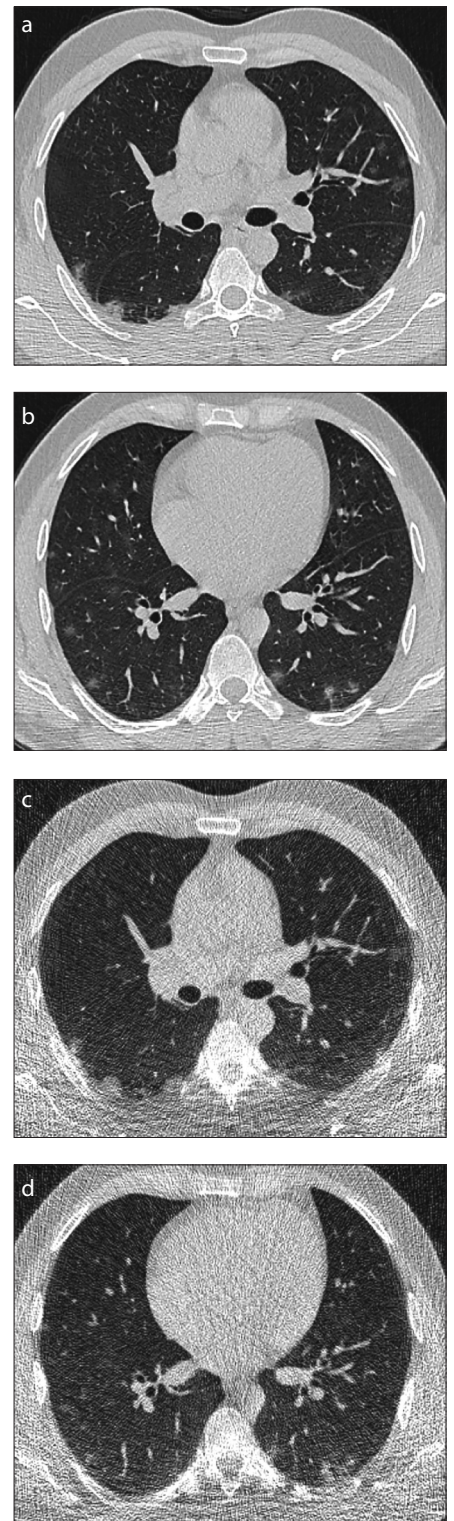


Figure 5. a–d. Axial standard (a, b) and low-dose (c, d) CT images of a 32-year-old male presenting with dyspnea, cough, and fever for two days. Standard-dose images (a, b) show typical early COVID-19 findings with bilateral ground-glass opacities. Some of these opacities are hard to detect even for experienced radiologists on low-dose images (c, d) and some of them are completely undetectable. Dose length product was 230.83 mSv·cm during standard-dose scan and 15.54 mSv·cm during low-dose scan.

**Table 3.** Categorical findings in study group (n=740) for each dose protocol, number of matching diagnoses and statistical significance of the differences

Findings	Standard-dose n (%)	Low-dose n (%)	Matching diagnoses n	Significance p
Peripheral bilateral/multilobar GGO	150 (20.3)	118 (15.9)	688	<0.001
Multifocal rounded GGO	15 (2.0)	13 (1.8)	732	0.727*
Reverse halo	28 (3.8)	13 (1.8)	719	0.001
Consolidation	97 (13.1)	85 (11.5)	708	0.052*
Crazy-paving	60 (8.1)	11 (1.5)	691	<0.001
Bronchovascular enlargement	125 (6.9)	22 (3.0)	637	<0.001
Air bronchogram	58 (7.8)	24 (3.2)	696	<0.001
Bronchial deformation	19 (2.6)	3 (0.4)	724	<0.001
Multifocal/diffuse/perihilar/unilateral GGO with or without consolidation	79 (9.5)	40 (5.4)	688	<0.001
Nonrounded and nonperipheral few very small GGOs	3 (0.4)	0 (0.0)	737	0.250*
Lobar/segmental consolidation without GGO	5 (0.7)	7 (0.9)	736	0.625*
Small discrete nodules, tree in bud/centrilobular	67 (9.1)	28 (3.8)	697	<0.001
Cavitation	0 (0.0)	0 (0.0)	740	NA
Effusion	29 (3.9)	7 (0.9)	714	<0.001
Lymphadenopathy	19 (2.6)	0 (0.0)	721	<0.001
Pneumothorax	1 (0.1)	0 (0.0)	739	1.000*
Diffuse fibrosis	24 (3.2)	1 (0.1)	717	<0.001
No features to suggest pneumonia	481 (65.0)	551 (74.5)	658	<0.001

GGO, ground-glass opacity; NA, not available.

\*  $p > 0.01$  (difference between low-dose and standard-dose is not significant for the finding in question).

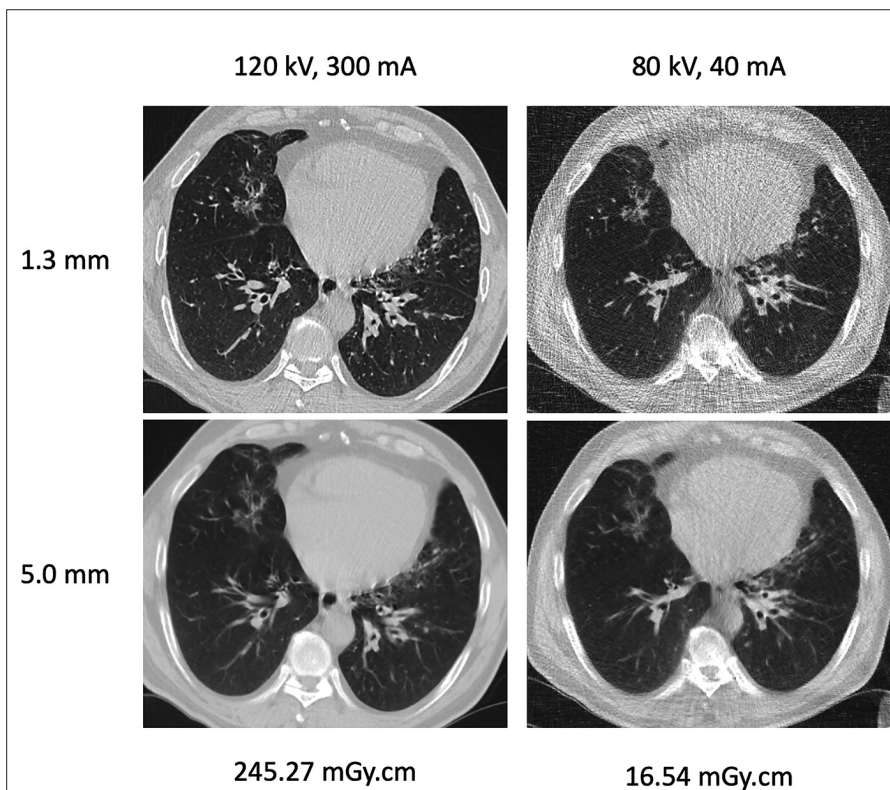


**Figure 6.** Axial standard-dose and low-dose, 1.3 mm and 5 mm CT images of a 49-year-old male presenting with fever (37.8°C) and low oxygen saturation (94%). Parenchymal lesions have much higher contrast than ground-glass opacities seen in Fig. 3 and they may be easily detected at both standard and low-dose protocols, using thick or thin sections.

sis, its sensitivity is as low as 60%–70% and results may also be considerably delayed (6). Moreover, its sensitivity is dependent on time since exposure to the virus, with a false negative rate of 100% on the first day, dropping to 67% on the fourth day (20). As patients may become a source of infection even during the incubation period (2), CT has gained importance as a surrogate diagnostic method due to its high sensitivity of up to 98% (6, 21, 22). CT imaging is not only used during the initial presentation and diagnosis but also in monitoring the progression of the disease, resulting in consecutive scans within a short time frame (7, 23, 24). Such practice may significantly increase the cumulative radiation dose and may potentially increase the overall risk for late stochastic effects. Repeated scans may also have a damaging effect on blood lymphocytes, which were found to be reduced in some patients with COVID-19 (25, 26). The patient dose, therefore, became a focus of interest during the pandemic. On that context, Dangis et al. (22) have retrospectively studied 192 symptomatic patients to evaluate the reliability of low-dose CT in the diagnosis. They have found that even low-dose CT has performed better in diagnosis com-

**Table 4.** Frequency and percentage of final categorical diagnosis and matching diagnoses for each protocol

COVID-19 category	Standard-dose	Low-dose	Matching diagnoses
	n (%)	n (%)	n (%)
Typical	161 (21.8)	125 (16.9)	116 (15.7)
Indeterminate	64 (8.6)	37 (5.0)	23 (3.1)
Atypical	29 (3.9)	24 (3.2)	9 (1.2)
Negative	486 (65.7)	554 (74.9)	478 (64.6)
Total	740 (100.0)	740 (100.0)	626 (84.6)

**Table 5.** Crosstabulations of categorical diagnosis according to standard and low-dose protocols

		Low-dose			
		Typical	Indeterminate	Atypical	Negative
Standard-dose	Typical	116	13	6	26
	Indeterminate	2	23	9	30
	Atypical	0	0	9	20
	Negative	7	1	0	478

pared with RT-PCR. Our results for low-dose CT are higher than their results in terms of sensitivity (86.7% vs. 90%) even though many of our patients had shorter interval between the occurrence of their symptoms and the scanning than their patients. The higher sensitivity of the present study was most possibly due to the use of a structured reporting format. Nevertheless, the time interval between the occurrence of symptoms and scanning is still crucial in deciding whether low-dose or standard-dose is to be used as such difference may cause substantial difference in lesion detectability. If the interval is as long as two to three weeks, there may be no significant difference between standard-dose and low-dose scans regarding the detection of COVID-19 pneumonia (27).

Although the sensitivity of low-dose CT, as shown in this study, is relatively high, there are certain differences between standard-dose and low-dose scans regarding individual elements of the structured reporting. Of these, GGO is the main focus of interest in dose-lowering studies (13, 27). This is because of GGO's high occurrence in COVID-19 and its low contrast that is close to normal lung tissue, making its observation difficult if the image noise is increased (28) (Fig. 6). GGOs were actually subjected to dose lowering attempts long before this pandemic. Such attempts has formed a basis for protocols that are known as low-dose CT (29–31). Low-dose CT was actually

developed to screen and follow the pulmonary nodules. These nodules, whether solid or subsolid, can be observed as GGOs. GGOs on the other hand may represent premalignant and malignant lesions that makes their detection crucial (32, 33). Since this task necessitates large-scale screening and follow-up of nonsymptomatic population, low-dose CT has been widely used for such lesions (34, 35). However, even after its success was shown by the National Lung Screening Trial, there remained controversies on the effect of dose reducing techniques in detecting GGOs (28, 36). Our findings support the studies with unfavorable outcome as we have found significant differences between high and low-dose studies regarding certain GGO patterns (Table 3).

Dose-lowering strategies are mainly based on reducing the tube current because many studies have already shown that this method can effectively reduce the CT radiation (37). The use of modern reconstruction technologies are of paramount importance to preserve the final image quality during such attempts. By using an adaptive statistical iterative reconstruction (ASIR) technology, we were able to reduce the dose by 92%. Different reconstruction technologies may result in different dose levels and dose reduction ratios. As an example, researchers that used KARL 3D technology have remained on the very high side of patient dose at both standard and

low dose studies (mean, 360.50 mGy-cm and 87.25 mGy-cm) compared with our study (median, 189.98 mGy-cm and 15.59 mGy-cm) and were able to reduce the dose by only 76%. ASIR has enabled us to effectively reduce standard deviation for pixel noise, allowing a substantially reduced mA in the acquisition of diagnostic image and reducing the dose without jeopardizing low-contrast. However, such benefits largely depends on the clinical task and the patient size. Therefore, appropriate dose and techniques to achieve confident diagnoses should be determined on the basis of patients' and clinicians' particular needs. Thus, the major limitation of the study is the use of a single set of low-dose scanning protocol, although it was globally recommended by the manufacturer. Further studies with slightly higher tube currents may improve the diagnostic ability of low dose scanning while keeping radiation exposure levels at the minimum.

In conclusion, this study showed the presence of significant difference in the detectability of individual CT findings (i.e., individual elements of structured reporting system) of COVID-19 pneumonia, especially GGO-related findings, between the standard and low-dose scans. Based on our findings, and within the technical parameters outlined above, low-dose scans may not be used for the initial imaging of patients during the pandemic where higher sensitivity is preferred. However, low-dose scans still have substantial intertest reliability in diagnosing COVID-19 and high specificity when combined with the structured reporting system of RSNA and may be used in follow-up of COVID-19 patients with prior CT scans, although this hypothesis requires further study.

#### Conflict of interest disclosure

The authors declared no conflicts of interest.

#### References

1. Chan JF, Yuan S, Kok KH, To KKW, Chu H, Yang J. A familial cluster of pneumonia associated with the 2019 novel coronavirus indicating person-to-person transmission: a study of a family cluster. *Lancet* 2020; 395:514–523. [Crossref]
2. Rothe C, Schunk M, Sothmann P, et al. Transmission of 2019-nCoV infection from an asymptomatic contact in Germany. *N Engl J Med* 2020; 382:970–971. [Crossref]
3. Yang Y, Yang M, Shen C, et al. Evaluating the accuracy of different respiratory specimens in the laboratory diagnosis and monitoring the viral shedding of 2019-nCoV infections. *MedRxiv* 2020. Published online: February 17, 2020. [Crossref]

4. Ai T, Yang Z, Hou H, et al. Correlation of chest CT and RT-PCR testing for coronavirus disease 2019 (COVID-19) in China: a report of 1014 cases. *Radiology* 2020; 296:E32–E40. [\[Crossref\]](#)
5. de Jaegere TMH, Krdzalic J, Fassen BACM, Kwee RM. COVID-19 CT Investigators South-East Netherlands (CISEN) study group. Radiological Society of North America chest CT classification system for reporting COVID-19 pneumonia: interobserver variability and correlation with RT-PCR. *Radiol Cardiothorac Imaging* 2020; 2:e200213. [\[Crossref\]](#)
6. Fang Y, Zhang H, Xie J, et al. Sensitivity of chest CT for COVID-19: Comparison to RT-PCR. *Radiology* 2020; 296:E115–E117. [\[Crossref\]](#)
7. The World Health Organization. Use of chest imaging in COVID-19: a rapid advice guide. Geneva: World Health Organization; 2020 (WHO/2019-nCoV/Clinical/Radiology\_imaging/2020.1). License: CC BY-NC-SA 3.0 IGO.
8. National Research Council. Health risks from exposure to low levels of ionizing radiation: BEIR VII phase 2. Washington, DC: The National Academies Press, 2006.
9. Mettler FA, Bhargavan M, Faulkner K, et al. Radiologic and nuclear medicine studies in the United States and worldwide: frequency, radiation dose, and comparison with other radiation sources-1950-2007. *Radiology* 2009; 253:520–531. [\[Crossref\]](#)
10. European Commission, Food and Agriculture Organization of The United Nations, International Atomic Energy Agency, International Labour Organization, OECD Nuclear Energy Agency, Pan American Health Organization, United Nations Environment Programme, World Health Organization. Radiation Protection and Safety of Radiation Sources: International Basic Safety Standards, IAEA Safety Standards Series No. GSR Part 3, IAEA, Vienna, 2014.
11. Karakas HM, Katsari K, Pekar RB, et al. How to become a high-performance dose excellence center: Current concepts and applications of modern dose management system in SBU Fatih Sultan Mehmet Training and Research Hospital. *EuroSafe Imaging* 2019. Poster no: ESI-0059.
12. Simpson S, Kay FU, Abbara S, et al. Radiological Society of North America expert consensus statement on reporting chest CT findings related to COVID-19. Endorsed by the Society of Thoracic Radiology, the American College of Radiology, and RSNA. *Radiol Cardiothorac Imaging* 2020; 35:219–227. [\[Crossref\]](#)
13. Aslan S, Bekçi T, Çakır IM, Ekiz M, Yavuz I, Şahin AM. Diagnostic performance of low-dose chest CT to detect COVID-19: A Turkish population study. *Diagn Interv Radiol* 2021; 27:181–187. [\[Crossref\]](#)
14. Rubin GD, Ryerson CJ, Haramati LB. The role of chest imaging in patient management during the COVID-19 pandemic: a multinational consensus statement from the Fleischner Society. *Radiology* 2020; 296:172–180. [\[Crossref\]](#)
15. AAPM Task Group 204. AAPM Report No. 204 - Size-specific dose estimates (SSDE) in pediatric and adult body CT examinations. College Park: American Association of Physicists in Medicine; 2011.
16. Karakas HM, Cavli B, Tekin H, et al. Computed tomography dose reference levels (DRLs) at various levels of hospitals in Istanbul: secondary public, tertiary public, pediatric tertiary public, and university hospitals' experiences. *EuroSafe Imaging* 2019. Poster no: ESI-0026.
17. European Commission. Radiation protection N° 180. Diagnostic reference levels in thirty-six European countries. Directorate-General for Energy Directorate D - Nuclear Safety & Fuel Cycle Unit D3 - Radiation Protection, 2014.
18. Ye Z, Zhang Y, Wang Y, Huang Z, Song B. Chest CT manifestations of new coronavirus disease 2019 (COVID-19): a pictorial review. *Eur Radiol* 2020; 30:4381–4389. [\[Crossref\]](#)
19. Brennan P, Silman A. Statistical methods for assessing observer variability in clinical measures. *BMJ* 1992; 304:1491–1494. [\[Crossref\]](#)
20. Kucirka LM, Lauer SA, Laeyendecker O, Boon D, Lessler J. Variation in false-negative rate of reverse transcriptase polymerase chain reaction-based SARS-CoV-2 tests by time since exposure. *Ann Intern Med* 2020; 173:262–267. [\[Crossref\]](#)
21. National Health Commission of the People's Republic of China. The diagnostic and treatment protocol of COVID-19. China. 2020; Available at: [http://www.gov.cn/zhengce/zhengceku/2020-02/19/content\\_5480948.htm](http://www.gov.cn/zhengce/zhengceku/2020-02/19/content_5480948.htm). Accessed 3 Mar 2020.
22. Dangis A, Gieraerts C, Bruecker YD, et al. Accuracy and reproducibility of low-dose submillisievert chest CT for the diagnosis of COVID-19. *Radiol Cardiothorac Imaging* 2020; 2:e200196. [\[Crossref\]](#)
23. Kay F, Abbara S. The many faces of COVID-19: Spectrum of imaging manifestations. *Radiol Cardiothorac Imag* 2020; 2:e200037. [\[Crossref\]](#)
24. Guan CS, Wei LG, Xie RM, et al. CT findings of COVID-19 in follow-up: comparison between progression and recovery. *Diagn Interv Radiol* 2020; 26:301–307. [\[Crossref\]](#)
25. Bing L, Ma S, Xiaodong L. Experimental studies on injury effects of repeated computed tomography scan in mice. *Chin J Radiol Med Prot* 2014; 34:164–167.
26. Lu X, Gong W, Wang L, et al. Clinical features and high resolution CT imaging findings of preliminary diagnosis novel coronavirus pneumonia. *Chin J Radiol* 2020; 54:296–299.
27. Li J, Wang X, Huang X, Chen F, Zhang X, Liu Y. Application of CareDose 4D combined with Karl 3D technology in the low dose computed tomography for the follow-up of COVID-19. *BMC Med Imaging* 2020; 20:56. [\[Crossref\]](#)
28. Christie A, Charimo-Torrente J, Roychoudhury K, Vock P, Roos JE. Accuracy of low-dose computed tomography (CT) for detecting and characterizing the most common CT-patterns of pulmonary disease. *Eur J Radiol* 2013; 82:e142–150. [\[Crossref\]](#)
29. Hu S, Peng Z, He C, et al. Phantom study of the influence of CareDose 4D and Care KV on CT pulmonary ground glass nodule with respect to image quality and radiation dose. *Chin J Radiol Med Prot* 2019; 39:534–538.
30. Xu Y, Zhang TT, Hu ZH, et al. Effect of iterative reconstruction techniques on image quality in low radiation dose chest CT: a phantom study. *Diagn Interv Radiol* 2019; 25:442–450. [\[Crossref\]](#)
31. Xu Y, He W, Chen H, Hu Z, Li J, Zhang T. Impact of the adaptive statistical iterative reconstruction technique on image quality in ultra-low-dose CT. *Clin Radiol* 2013; 68:902–908. [\[Crossref\]](#)
32. Travis WD, Garg K, Franklin WA, et al. Evolving concepts in the pathology and computed tomography imaging of lung adenocarcinoma and bronchioloalveolar carcinoma. *J Clin Oncol* 2005; 23:3279–3287. [\[Crossref\]](#)
33. Lee HY, Lee KS. Ground-glass opacity nodules: histopathology, imaging evaluation, and clinical implications. *J Thorac Imaging* 2011; 26:106–118. [\[Crossref\]](#)
34. Henschke CI, Yip R, Yankelevitz DF, Smith JP. Computed tomography screening for lung cancer. *Ann Intern Med* 2013; 159:156–157. [\[Crossref\]](#)
35. Aberle DR, Berg CD, Black WC, et al. The National Lung Screening Trial: overview and study design. *Radiology* 2011; 258:243–253. [\[Crossref\]](#)
36. Kubo T, Ohno Y, Nishino M, et al. Low dose chest CT protocol (50mAs) as a routine protocol for comprehensive assessment of intrathoracic abnormality. *Eur J Radiol* 2016; 3:86–94. [\[Crossref\]](#)
37. Zhao F, Zeng YM, Peng G, et al. Correlation between the tube current and image noise in low-dose chest CT scan. *Chin J Radiol Med Prot* 2012; 32:100–103.